

Giant enhancement of negative friction by resonant coupling between localized surface phonon polaritons and graphene plasmonics

Kaipeng Liu(柳开鹏), Shuai Zhou(周帅), Shiwei Dai(戴士为), and Lixin Ge(葛力新)

Citation: Chin. Phys. B, 2025, 34 (**1**): 014202. DOI: 10.1088/1674-1056/ad886c
Journal homepage: http://cpb.iphy.ac.cn; http://iopscience.iop.org/cpb

What follows is a list of articles you may be interested in

Tunable artificial plasmonic nanolaser with wide spectrum emission operating at room temperature

Peng Zhou(周鹏), Jia-Qi Guo(郭佳琦), Kun Liang(梁琨), Lei Jin(金磊), Xiong-Yu Liang(梁熊玉), Jun-Qiang Li(李俊强), Xu-Yan Deng(邓绪彦), Jian-Yu Qin(秦建宇), Jia-Sen Zhang(张家森), and Li Yu(于丽)
Chin. Phys. B, 2024, 33 (**5**): 054210. DOI: 10.1088/1674-1056/ad2dca

Giant and controllable Goos—Hänchen shift of a reflective beam off a hyperbolic metasurface of polar crystals

Tian Xue(薛天), Yu-Bo Li(李宇博), Hao-Yuan Song(宋浩元), Xiang-Guang Wang(王相光), Qiang Zhang(张强), Shu-Fang Fu(付淑芳), Sheng Zhou(周胜), and Xuan-Zhang Wang(王选章)
Chin. Phys. B, 2024, 33 (**1**): 014207. DOI: 10.1088/1674-1056/acdac2

Omnidirectional and compact Tamm phonon-polaritons enhanced mid-infrared absorber

Xiaomin Hua(花小敏), Gaige Zheng(郑改革), Fenglin Xian(咸冯林), Dongdong Xu(徐董董), and Shengyao Wang(王升耀)
Chin. Phys. B, 2021, 30 (**8**): 084202. DOI: 10.1088/1674-1056/abe22b

Narrowband perfect terahertz absorber based on polar-dielectrics metasurface

Meng-Meng Zhao(赵萌萌), Shu-Fang Fu(付淑芳), Sheng Zhou(周胜), Yu-Ling Song(宋玉玲), Qiang Zhang(张强), Yong-Qi Yin(尹永琦), Yu-Tian Zhao(赵玉田), Hong Liang(梁红), Xuan-Zhang Wang(王选章)
Chin. Phys. B, 2020, 29 (**5**): 054210. DOI: 10.1088/1674-1056/ab81fa

Design and optimization of a SiC thermal emitter/absorber composed of periodic microstructures based on a non-linear method

Wang Wei-Jie (王卫杰), Zhao Zhen-Guo (赵振国), Zhao Yi (赵艺), Zhou Hai-Jing (周海京), Fu Ce-Ji (符策基)
Chin. Phys. B, 2015, 24 (**9**): 094213. DOI: 10.1088/1674-1056/24/9/094213

Giant enhancement of negative friction by resonant coupling between localized surface phonon polaritons and graphene plasmonics

Kaipeng Liu(柳开鹏)[1], Shuai Zhou(周帅)[1,3], Shiwei Dai(戴士为)[2], and Lixin Ge(葛力新)[1,†]

[1]*School of Physics and Electronic Engineering, Xinyang Normal University, Xinyang* 464000, *China*
[2]*College of Mathematics and Physics, Chengdu University of Technology, Chengdu* 610059, *China*
[3]*Department of Basic Courses, Zhengzhou University of Science and Technology, Zhengzhou* 450064, *China*

(Received 1 September 2024; revised manuscript received 1 October 2024; accepted manuscript online 18 October 2024)

Negative friction refers to a frictional force that acts in the same direction as the motion of an object, which has been predicted in terahertz (THz) gain systems [*Phys. Rev. B* **108** 045406 (2023)]. In this work, we investigate the enhancement of the negative friction experienced by nanospheres placed near a graphene substrate. We find that the magnitude of negative friction is related to the resonant coupling between the surface plasmon polaritons (SPPs) of the graphene and localized surface phonon polaritons (LSPhP) of nanospheres. We exam nanospheres consisted of several different materials, including SiO_2, SiC, ZnSe, NaCl, lnSb. Our results suggest that the LSPhP of NaCl nanospheres match effectively with the amplified SPPs of graphene sheets. The negative friction for NaCl nanospheres can be enhanced about one-to-two orders of magnitude compared to that of silica (SiO_2) nanospheres. At the resonant peak of negative friction, the required quasi-Fermi energy of graphene is lower for NaCl nanospheres. Our finds hold great prospects for the mechanical manipulations of nanoscale particles.

Keywords: quantum friction, surface phonon polaritons, surface plasmon polaritons, graphene

PACS: 42.50.Lc, 73.20.Mf, 62.20.Qp, 61.48.Gh

DOI: 10.1088/1674-1056/ad886c **CSTR:** 32038.14.CPB.ad886c

1. Introduction

In classical physics, friction is typically described as the resistance generated between two objects in contact due to electromagnetic interactions at their surfaces. In quantum physics, non-contact friction can also arise when two objects move relative to each other without direct contact,[1–3] which is caused by vacuum fluctuations and the Doppler effect, even at the absolute zero.[3] The quantum friction between two sliding objects have been investigated in a variety of configurations,[4–13] such as materials consisted of metal,[1,4] dielectric,[5,6] graphene,[7–9] topological materials,[10,11] space–time-modulated media,[12] etc. The quantum frictions were also predicted between moving atoms and plates.[13–16]

On the other side, the rotation of objects in vacuum would slow down its rotating speed due to the quantum friction.[17–19] As rotating nanoparticles approach a planar substrate, the friction torque can be amplified by several orders of magnitude at short separations,[20–23] because of the localized surface modes, such as surface plasmons polaritons (SPPs),[20] surface phonon polaritons (SPhPs),[20,21] magnon–polariton modes,[22] or hyperbolic modes.[23] When the substrate breaking parity symmetry or/and time-reversal symmetry, a dissipationless friction force was predicted for a rotating particle.[24,25] Levitation and rotating a nanoparticle at GHz speeds have been realized in recent experiments.[26–28] Moreover, the separation within a submicrometer scale between the rotating particles and the substrate was reported by Ju *et al.*[29] For the ceramic material of BST, the friction torque of nanospheres can be up to the order of 10^{-23} N·m due to the resonance of SPhPs at GHz frequencies.[30] Thanks to the low-frequency SPhPs in BST, the experimental detection of quantum friction was successfully observed and claimed by Li *et al.*[31]

Negative friction means that the frictional force acts in the same direction as the motion of an object, resulting in the object being accelerated rather than hindered.[32] Clearly, in a closed system, negative friction violates the law of energy conservation in thermodynamics. To realize negative friction, it is essential to introduce a gain medium, therefore the system can continuously acquire energy from an external source (such as an applied current or an external laser). Graphene sheets can serve as a terahertz gain medium when subjected to external pumping light or an electric bias.[33–35] In its gain state, the surface plasmon of graphene can be amplified by external pump, and transfer its momentum to the nanoparticles through vacuum interaction, leading to the exotic negative friction.

In this work, we investigate the enhancement of negative friction for rotating nanospheres near an active graphene sheet. The negative friction torque can be enhanced greatly

†Corresponding author. E-mail: lixinge@hotmail.com

© 2025 Chinese Physical Society and IOP Publishing Ltd. All rights, including for text and data mining, AI training, and similar technologies, are reserved.

by resonant coupling between the LSPhP of the nanoparticles and the SPPs of graphene. We compared the frictional torques of nanoparticles made from different materials. We find that the LSPhP of NaCl nanospheres matches effectively with the SPPs of graphene. The maximum value of the negative friction torque for NaCl nanospheres corresponds to a lower quasi-Fermi level and is increased by two orders of magnitude compared to silica (SiO_2) under the same conditions. At the end, the influences of relaxation time, temperature, and the separation on the enhancement of negative friction are discussed.

The structure of this paper is organized as follows: In Section 2, we describe the theoretical framework for the friction torque of rotating nanospheres and the dielectric model for the used materials. Transitioning to Section 3, we present the numerical results of negative friction for different nanospheres, with a detailed discussion on the resonant coupling between the LSPhP in nanospheres and the SPPs of graphene sheets. The parameters of systems such as the temperature, separation are also discussed.

2. Theoretical models

The schematic diagram of the system is shown in Fig. 1. A rotating nanosphere with a radius R is suspended in a vacuum. The distance from the center of the nanosphere to the substrate is d. The rotation axis of the nanosphere is parallel to the x-axis. According to the fluctuation–dissipation theorem, the friction torque of the nanosphere is given as follows:[20]

$$M_{\rm p} = -\frac{2\hbar}{\pi}\int_{-\infty}^{+\infty}[n_0(\omega-\Omega)-n_1(\omega)] \times \mathrm{Im}[\alpha(\omega-\Omega)]\,\mathrm{Im}[\overline{G}(\omega)]\,\mathrm{d}\omega, \tag{1}$$

where $\hbar$ is the reduced Planck constant, ω is the angular frequency of fluctuating photons, Ω is the angular frequency of the rotating nanosphere, $n_j(\omega) = [\exp(\hbar\omega/k_{\rm B}T_j)-1]^{-1}$ is the Bose–Einstein distribution function, T_j $(j=0,1)$ represents the temperature of the substrate and the nanosphere, $k_{\rm B}$ is the Boltzmann constant, $\alpha(\omega)$ is the polarizability of nanospheres, and $\overline{G}(\omega)$ is the Green's function. The polarizability and Green function can be expressed as

$$\alpha(\omega) = R^3\frac{\varepsilon_{\rm sp}(\omega)-1}{\varepsilon_{\rm sp}(\omega)+2}, \tag{2}$$

$$\overline{G}(\omega) = \frac{\mathrm{i}}{2}\int_0^{\infty} k_{||}\,\mathrm{d}k_{||}\,\mathrm{e}^{2\mathrm{i}k_z d}\left[\left(\frac{k_{||}^2}{k_z}-\frac{k_z}{2}\right)r_{\rm p}+r_{\rm s}\frac{k_0^2}{2k_z}\right], \tag{3}$$

where $\varepsilon_{\rm sp}(\omega)$ is the permittivity of nanosphere, $k_{||}$ and $k_z = \sqrt{k_0^2-k_{||}^2}$ represent the parallel and vertical wave vectors, $k_0 = \omega/c$ is the total wave vector with c being the velocity of light in the vacuum, $r_{\rm s}$ and $r_{\rm p}$ are the reflection coefficients for transverse electric (TE) and transverse magnetic (TM) modes, respectively. For a graphene sheet placed on a dielectric substrate, the reflection coefficients can be given by the following formula:[36,37]

$$r_{\rm s} = \frac{k_{1z}-k_{2z}-k_0\hat{\sigma}}{k_{1z}+k_{2z}+k_0\hat{\sigma}}, \tag{4}$$

$$r_{\rm p} = \frac{\varepsilon_1/k_{1z}-\varepsilon_2/k_{2z}-\hat{\sigma}/k_0}{\varepsilon_1/k_{1z}+\varepsilon_2/k_{2z}+\hat{\sigma}/k_0}, \tag{5}$$

where $\varepsilon_1 = 1$, $\varepsilon_2 = \varepsilon_{\rm sub}$, $k_{jz} = \sqrt{\varepsilon_j k_0^2 - k_m^2}$, $(j=1,2)$, $\hat{\sigma} = \sigma/\eta_0$ represents the normalized conductivity of graphene, and η is the impedance of free space. The graphene conductivity is contributed by the intra-band and inter-band transitions, and the expression is written as[38,39]

$$\sigma(\omega) = \frac{e^2}{\hbar}\frac{\mathrm{i}2k_{\rm B}T}{\pi\hbar(\omega+\mathrm{i}/\tau)}\ln\left[1+\exp\left(\frac{\mu_{\rm F}}{k_{\rm B}T}\right)\right] + \frac{e^2}{4\hbar}\tanh\left(\frac{\hbar\omega-2\mu_{\rm F}}{4k_{\rm B}T}\right) + \frac{\mathrm{i}e^2\hbar\omega}{\pi\hbar}\int_0^{\infty}\frac{g(x)-g(\hbar\omega/2)}{(\hbar\omega)^2-4x^2}\,\mathrm{d}x, \tag{6}$$

where $\mu_{\rm F}$ is the quasi-Fermi energy, depending on the intensity of photoexcitation or electrical bias, e is the charge of an electron, and τ is the momentum relaxation time of the charge carriers. The effective temperature T is assumed to be the lattice temperature. The auxiliary function $g(x)$ is given by

$$g(x) = \frac{\sinh(x/k_{\rm B}T)}{\cosh(\mu_{\rm F}/k_{\rm B}T)+\cosh(x/k_{\rm B}T)}. \tag{7}$$

The dielectric constant of the nanospheres can be expressed using the Lorenz's model[40]

$$\varepsilon(\omega) = \varepsilon_\infty + \sum_{l=1}^{N}\frac{\varepsilon_\infty(\omega_{\rm LO,l}^2-\omega_{\rm TO,l}^2)}{\omega_{\rm TO,l}^2-\omega^2-\mathrm{i}\omega\gamma_l}, \tag{8}$$

where ε_∞ is the permittivity in the high-frequency limit, $\omega_{\rm LO,l}$ is the longitudinal polar-optic phonon frequency, $\omega_{\rm TO,l}$ is the transverse polar-optic phonon frequency, γ_l is the damping coefficient. The Lorenz parameters for different materials are listed in Table 1.[40]

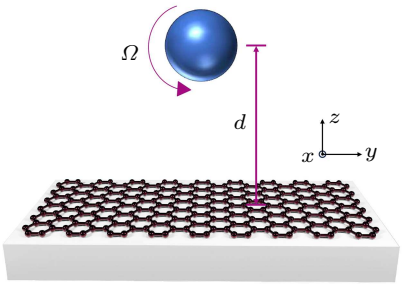


Fig. 1. Schematic view of the system under study. The rotating nanospheres is suspended in a vacuum. The semi-infinite dielectric plate is covered by graphene, which can be a gain medium under an external pumping light or electric bias. The nanosphere rotates around the x-axis, and the distance from the center of the nanosphere to substrate is d.

Table 1. Lorenz parameters for different materials.[40]

Sem.[a]	ε_∞	$\omega_{TO} \times 10^{12}$ (rad/s)	$\omega_{LO} \times 10^{12}$ (rad/s)	$\gamma \times 10^{12}$ (rad/s)
ZnSe	5.4	39.00	46.34	0.70
lnSb	15.7	33.91	36.17	0.57
SiC	6.7	149.37	182.52	0.90
NaCl	2.22	30.90	50.37	1.20
SiO_2	2.09	$6\pi\times\{11.67, 10.64, 10.58, 7.99, 4.34\}$	$6\pi\times\{11.86, 11.12, 11.06, 8.14, 5.25\}$	$6\pi\times\{0.0443, 0.1553, 0.0042, 0.1294, 0.5414\}$

3. Results and discussion

The friction torque exerted on the nanosphere is linked to the local photonic density of states (LDOS) at its location, which is proportional to $\mathrm{Im}[G(\omega)]$. As illustrated in Fig. 2, the $\mathrm{Im}[G(\omega)]$ can be positive or negative, depending upon the magnitude of μ_F in graphene. We set the momentum relaxation time $\tau = 1$ ps in the calculations, which is consistent with the experiment results.[41] For a low quasi-Fermi energy, the graphene sheet behaves as a lossy material. Hence, $\mathrm{Im}[G(\omega)]$ is positive throughout the entire spectrum. This positive LDOS represents the action of hinders, as dictated by the fluctuation–dissipation theorem. It is noteworthy that as the μ_F surpasses 16 meV, the resonance peaks of $\mathrm{Im}[G(\omega)]$ turns to be negative values.[32] The negative LDOS is attributed to the amplified SPPs in graphene, which can lead to a reversal of the friction torque. The resonant frequencies of $\mathrm{Im}[G(\omega)]$ increases monotonously with μ_F as shown in the inset of Fig. 2. When μ_F is smaller than 100 meV, the resonance frequency of $\mathrm{Im}[G(\omega)]$ is lower than about 11 THz.

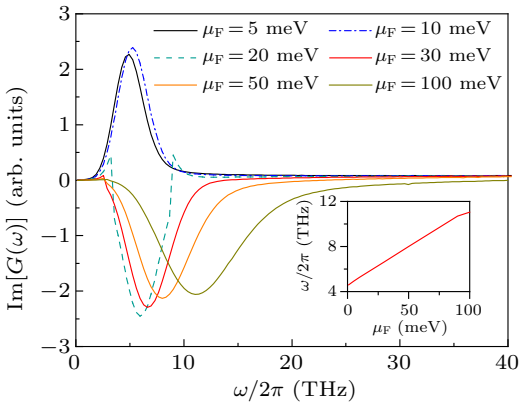


Fig. 2. The imaginary part of the Green's function via the photon frequency under different quasi-Fermi energies of graphene sheet. The permittivity of the dielectric substrate is $\varepsilon_{sub} = 1.5$. The inset shows the resonant frequencies of $\mathrm{Im}[G(\omega)]$ as a function of quasi-Fermi energy. Here, we set the distance $d = 300$ nm and the temperature $T = 300$ K.

The real part of permittivities given by the Lorentz model are shown in Fig. 3(a) for different materials. Interestingly, the Reststrahlen effect (corresponding to $\mathrm{Re}[\varepsilon] < 0$),[40] due to the strong interaction between electromagnetic waves and the lattice vibrations (phonons) in material, can be found at THz and infrared frequencies. The Reststrahlen bands start from about 5 THz for materials of NaCl, ZnSe, and InSb, whereas the start frequencies are larger than 10 THz for material of SiO_2 and SiC. The polarizability of nanospheres $\alpha(\omega)$ for various materials are shown in Fig. 3(b). The $\alpha(\omega)$ exhibits resonance response, corresponding to the excitation of LSPhP for $\mathrm{Re}\{\varepsilon(\omega)\} = -2$, as indicated from Eq. (2). As expected, SiO_2 shows four resonance peaks, whereas other materials display a single resonance peak. For the materials of NaCl, ZnSe, and InSb, the resonance frequencies are lower than 10 THz, and the $\alpha(\omega)$ of NaCl nanosphere is the strongest. As we can see, the polarizability resonances for nanospheres composed of phononic materials appear at THz or mid-infrared regime, while the resonances appear at visible and near-infrared frequencies for metallic nanoparticles.[42,43]

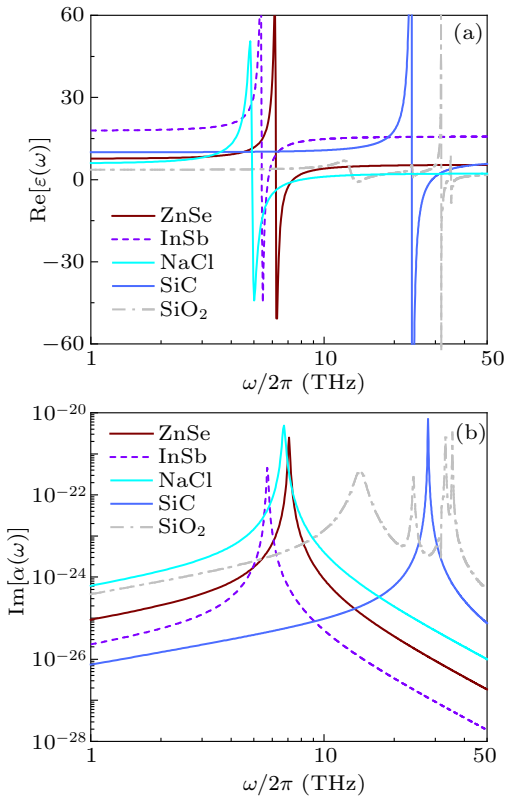


Fig. 3. (a) The real part of permittivity via angular photon frequency for different materials. (b) The imaginary part of polarizability of nanospheres. The radius $R = 75$ nm.

Figure 4(a) shows the friction torque of nanospheres for different materials. At the beginning, the friction torque is positive for all presented materials when μ_F increases from zero. As μ_F increases further, the friction torque turns from

positive to negative sharply. Clearly, there is zero-friction phenomenon for specific value of μ_F, wherein the quantum friction that hinders object movement disappears. On the other side, the magnitudes of negative friction are strongly dependent on the materials of nanospheres. The negative friction torque M_p is weak for SiC, which is attributed to the mismatch between the LSPhP of SiC and the graphene SPPs. The negative M_p for SiO_2 increases with μ_F, and the torque is about -4×10^{-28} N·m at $\mu_F = 100$ meV. For InSb nanospheres, the negative M_p is comparable with that of SiO_2, whereas the maximum of the M_p appears at a much lower μ_F (about 35 meV). Remarkably, the giant enhancement of negative friction torque is revealed for ZnSe and NaCl nanospheres. The maximum values of negative torque are approximately -1.6×10^{-27} N·m at $\mu_F = 40$ meV for ZnSe, which has been enhanced several times compared the negative torque of SiO_2 nanosphere at $\mu_F = 100$ meV. The enhancement of negative friction is most prominent for NaCl. The peak of negative M_p is about -6.5×10^{-27} N·m at the $\mu_F = 36$ meV. For a comparison, the negative friction torque of SiO_2 nanosphere is only about -1.1×10^{-28} N·m at $\mu_F = 36$ meV, and the friction torque of NaCl is enlarged by dozens of times. The giant enhancement is attributed to the strong coupling between the LSPhP of NaCl nanospheres and the SPPs of graphene.

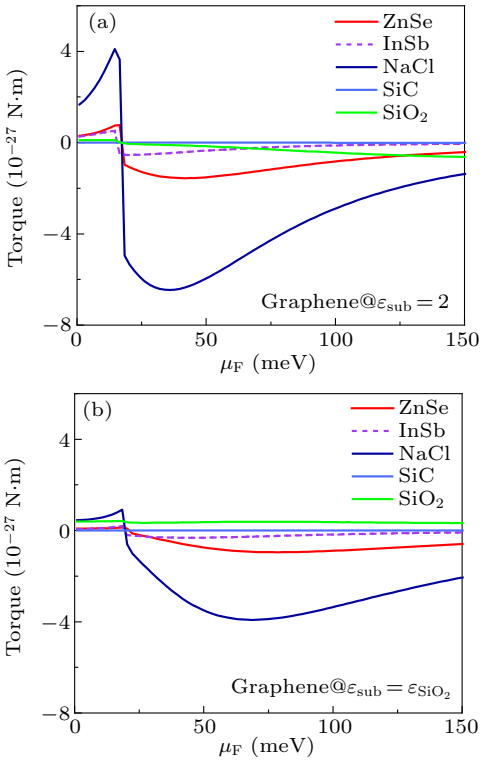


Fig. 4. (a) The friction torque on nanospheres as a function of quasi-Fermi energy of graphene sheet. The substrate composed of a graphene sheet covered on a semi-infinite dielectric plate with $\varepsilon_{sub} = 2$. (b) The substrate is graphene sheet placed on a semi-infinite SiO_2 plate. We set the temperature $T = 300$ K, the radius $R = 75$ nm, the rotation frequency $\Omega/2\pi = 5$ GHz, and $d = 300$ nm.

The coupling of the SPhPs and SPPs produces the mixed mode, called the surface plasmon–phonon–polaritons (SPPPs).[44] The substrate consists of graphene-covered SiO_2 would enrich the phenomena of friction torque, due to the coupling of the SPhPs of SiO_2 and graphene SPPs. The friction torque via the quasi-Fermi energy is shown in Fig. 4(b). The friction torque for SiO_2 nanospheres is always positive. This is because the LSPhPs in SiO_2 nanospheres predominantly couple with the SPhPs of the SiO_2 plate, while their coupling with graphene plasmon is secondary. By contrast, strong negative friction torque still persists for NaCl and ZnSe nanospheres. This is because the LSPhPs in NaCl and ZnSe nanospheres couple primarily with the amplified SPPs in graphene, rather than with the SPhPs of SiO_2 plate. The results show that the peaks of negative friction torque decrease slightly compared with the case of Fig. 4(a), and the μ_F for maximum negative friction shifts to a relatively large value.

Next, we consider the friction torque changed with the relaxation time τ, which is an important parameter of active graphene sheet. The friction torque of NaCl nanospheres under different relaxation time is shown in Fig. 5(a). The results suggest that the relaxation time plays an important role in the negative friction torque. The friction torque for $\tau = 0.4$ ps is almost the same as that of $\tau = 1$ ps. As the relaxation time reduces to 0.2 ps, the friction torque becomes negative only for a specific window of μ_F. When the τ declines to 0.1 ps, the friction torque become positive over all range of μ_F. Practically, the relaxation time $\tau \sim 1$ ps at room temperature was experimentally reported in multilayer epitaxial graphene.[45,46] Moreover, the relaxation time τ larger than 1 ps has been observed in optical pumped graphene.[47]

A higher temperature could enhance the negative friction torque further as shown in Fig. 5(b), where we fix the $\mu_F = 35$ meV. As shown before, the friction torque is positive when the relaxation time is as small as 0.1 ps. When the parameter τ increases, the friction torque increases slightly, and then turns to negative values sharply. The sign transition from positive to negative is sharp, wherein the relaxation time for the transition is dependent on the temperature. The larger the temperature, the larger of the relaxation time required at the transition. For example, the minimum relaxation time for negative friction is about 0.15 ps at 200 K, whereas the time is about 0.4 ps at temperature 500 K. Interestingly, the negative friction is almost unchanged when the relaxation time is larger than the transition one. The magnitude of negative friction for 500 K is about 2 and 3 times of those for 300 K and 200 K, respectively.

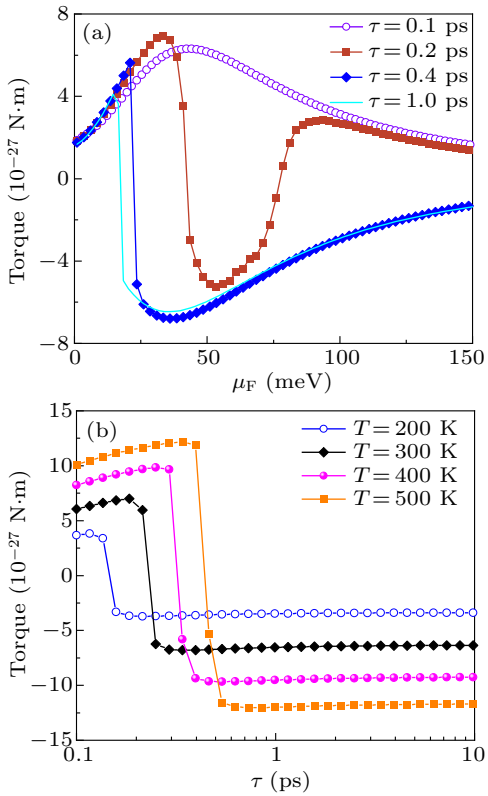


Fig. 5. (a) The friction torque on NaCl nanospheres under different relaxation time. The temperature $T = 300$ K. (b) The friction torque on NaCl nanospheres as a function of relaxation time under different temperatures. We set $\mu_F = 35$ meV. Other parameters are kept the same as those in Fig. 4(a).

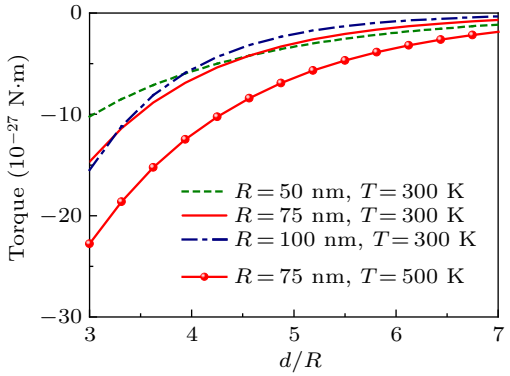


Fig. 6. The friction torque on NaCl nanospheres as a function of normalized separation. We set $\mu_F = 35$ meV, and other parameters are kept the same as those in Fig. 4(a).

Finally, we consider the influence of the separation on friction torque under different configurations, as shown in Fig. 6. For different radii of NaCl nanospheres, the magnitude of negative friction declines with increasing the separation. When the separation $d \sim 3R$, the negative friction torque at 300 K is at the order of 10^{-26} N·m, and it is two order larger than that of air resistance with pressure 10^{-10} Torr (1 Torr = 1.33322×10^2 Pa).[32] Compared with the case of 300 K, the negative friction torque for radius of 75 nm can be enhanced further at 500 K. It is worth mentioning that the separation in this work is set under the condition of $d > 3R$, and it is possible to further enhance the negative friction at even closer distances ($d < 3R$). However, the electric-dipole model for rotating nanospheres may not be applicable at extremely close distances, and a more accurate model needs to be developed.

4. Conclusion and perspectives

In summary, this work demonstrates the giant enhancement of negative friction via resonant coupling between LSPhP of nanosphere and SPPs of graphene sheets. For comparisons, the rotating nanosphere consisted of different materials are investigated. We found that the LSPhPs in NaCl nanospheres match effectively with the graphene SPPs. The magnitude of negative friction for NaCl is enhanced with one-to-two orders compared to that of SiO_2. Moreover, the quasi-Fermi energy at the maximum of negative friction is lower for NaCl, which is highly preferred for real experiments. The influences of the relaxation time, temperature, and the separation on the enhancement of negative friction have been discussed. Our concepts of negative friction and its enhancement are also expected to be found in other gain materials, such as semiconductors, which would be a meaningful direction in future.

Acknowledgements

Project supported by the National Natural Science Foundation of China (Grant No. 11804288) and the Key Scientific Research Project of Higher Education Institutions in Henan Province, China (Grant No. 20231205164502999).

References

[1] Volokitin A I and Persson B N J 2007 *Rev. Mod. Phys.* **79** 1291
[2] Reiche D, Intravaia F and Busch K 2022 *APL Photon.* **7** 030902
[3] Pendry J B 1997 *J. Phys.: Condens. Matter* **9** 10301
[4] Volokitin A I and Persson B N J 2003 *Phys. Rev. Lett.* **91** 106101
[5] Volokitin A I 2019 *JETP Lett.* **110** 397404
[6] Volokitin A I and Persson B N J 2016 *Phys. Rev. B* **93** 035407
[7] Farias M B, Fosco C D, Lombardo F C and Mazzitelli F D 2017 *Phys. Rev. D* **95** 065012
[8] Wang T B, Liu N H, Liu J T and Yu T B 2014 *Eur. Phys. J. B* **87** 15
[9] Volokitin A I and Persson B N J 2011 *Phys. Rev. Lett.* **106** 094502
[10] Farias M B, Kort-Kamp W J M and Dalvit D A R 2018 *Phys. Rev. B* **97** 161407
[11] Yu T, Luo R, Wang T B, Zhang D J, Liu W X, Yu T B and Liao Q H 2022 *Nanomaterials* **12** 1148
[12] Oue D, Ding K and Pendry J B 2023 *Phys. Rev. A* **107** 063501
[13] Intravaia F, Oelschläger M, Reiche D, Dalvit D A R and Busch K 2019 *Phys. Rev. Lett.* **123** 120401
[14] Guo X, Milton K A, Kennedy G and Pourtolami N 2023 *Phys. Rev. A* **107** 062812
[15] Reiche D, Dalvit D A R, Busch K and Intravaia F 2017 *Phys. Rev. B* **95** 155448
[16] Fernández A and Fosco C D 2023 *Phys. Rev. D* **108** 116010
[17] Manjavacas A and García de Abajo F J 2010 *Phys. Rev. Lett.* **105** 113601
[18] Manjavacas A and García de Abajo F J 2010 *Phys. Rev. A* **82** 063827
[19] Sanders S, Kort-Kamp W J M, Dalvit D A R and Manjavacas A 2019 *Commun. Phys.* **2** 71
[20] Zhao R, Manjavacas A, García de Abajo F J and Pendry J B 2012 *Phys. Rev. Lett.* **109** 123604

[21] Manjavacas A, Rodríguez-Fortuño F J, García de Abajo F J and Zayats A V 2017 *Phys. Rev. Lett.* **118** 133605

[22] Khosravi F, Sun W, Khandekar C, Li T and Jacob Z 2024 *New J. Phys.* **26** 053006

[23] Wang T B, Zhou Y, Mu H Q, Shehzad K, Zhang D J, Liu W X and Liao Q H 2022 *Nanotechnology* **33** 245001

[24] Jiang Q D and Wilczek F 2019 *Phys. Rev. B* **99** 165402

[25] Yu T, You W, Wang T, Yu T B and Liao Q H 2023 *Results Phys.* **52** 106902

[26] Ahn J, Xu Z, Bang J, Ju P, Gao X and Li T 2020 *Nat. Nanotechnol.* **15** 89

[27] Ahn J, Xu Z, Bang J, Deng Y H, Hoang T M, Han Q, Ma R and Li T 2018 *Phys. Rev. Lett.* **121** 033603

[28] Jin Y, Yan J, Rahman S J, Li J, Yu X and Zhang J 2021 *Photon. Res.* **9** 1344

[29] Ju P, Jin Y, Shen K, Duan Y, Xu Z, Gao X, Ni X and Li T 2023 *Nano Lett.* **23** 10157

[30] Xu Z, Jacob Z and Li T 2020 *Nanophotonics* **10** 537

[31] Xu Z, Ju P, Shen K, Jin Y, Jacob Z and Li T 2024 arXiv: 2403.06051 [quant-ph]

[32] Ge L 2023 *Phys. Rev. B* **108** 045406

[33] Otsuji T, Popov V and Ryzhii V 2014 *J. Phys. D: Appl. Phys.* **47** 094006

[34] Fateev D V, Polischuk O V, Mashinsky K V, Moiseenko I M, Morozov M Y and Popov V V 2021 *Phys. Rev. Appl.* **15** 034043

[35] Chen P Y and Jung J 2016 *Phys. Rev. Appl.* **5** 064018

[36] Kotov O V and Lozovik Y E 2017 *Phys. Rev. B* **96** 235403

[37] Zhan T, Shi X, Dai Y, Liu X and Zi J 2013 *J. Phys.: Condens. Matter* **25** 215301

[38] Dubinov A A, Aleshkin V Y, Mitin V, Otsuji T and Ryzhii V 2011 *J. Phys.: Condens. Matter* **23** 145302

[39] Popov V V, Polischuk O V, Davoyan A R, Ryzhii V, Otsuji T and Shur M 2020 *Graphene-Based Terahertz Electronics and Plasmonics* (New York: Jenny Stanford Publishing) pp. 587–601

[40] Foteinopoulou S, Devarapu G C R, Subramania G S, Krishna S and Wasserman D 2019 *Nanophotonics* **8** 2129

[41] Gierz I, Petersen J C, Mitrano M, Cacho C, Turcu I E, Springate E, Stöhr A, Köhler A, Starke U and Cavalleri A 2013 *Nat. Mater.* **12** 1119

[42] Qi Y Z, Jiang Q, Xiang H and Han D Z 2023 *Chin. Phys. B* **32** 104202

[43] Zhu X, Meng B, Wang D, Chen X, Liao L, Jiang M and Wei Z 2022 *Chin. Phys. B* **31** 047801

[44] Xue T, Li Y B, Song H Y, Wang X G, Zhang Q, Fu S F, Zhou S and Wang X Z 2023 *Chin. Phys. B* **33** 014207

[45] Tan Y W, Zhang Y, Bolotin K, Zhao Y, Adam S, Hwang E H, Sarma S D, Stormer H L and Kim P 2007 *Phys. Rev. Lett.* **99** 246803

[46] Orlita M, Faugeras C, Plochocka P, Neugebauer P, Martinez G, Maude D K, Barra A L, Sprinkle M, Berger C, de Heer W A and Potemski M 2008 *Phys. Rev. Lett.* **101** 267601

[47] Dawlaty J M, Shivaraman S, Chandrashekhar M, Rana F and Spencer M G 2008 *Appl. Phys. Lett.* **92** 042116